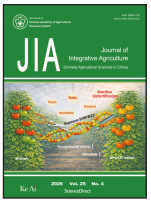
Journal of Integrative Agriculture 2026, 25(4): 1544–1555

KeAi
CHINESE ROOTS
GLOBAL IMPACT

Available online at ScienceDirect

Journal of Integrative Agriculture



RESEARCH ARTICLE

Elucidating the mechanisms of *Fusarium oxysporum* f. sp. *tuberosi* inhibition using functionalized multi-walled carbon nanotubes: A comprehensive analysis of biophysical and molecular interactions

Sadia Manzoor[1#], Asma Irshad[2], Saira Azam[3], Ijaz Ali[7], Ayesha Latif[3], Abdul Qayyum Rao[3], Samina Hassan[4], Ahmad Ali Shahid[3], Muhammad Danish Ali[5, 6#], Ameni Brahmia[8]

[1] *Centre for Applied Molecular Biology, University of the Punjab, Thokar Niaz Baig Lahore 53700, Pakistan*
[2] *School of Biochemistry & Biotechnology, University of the Punjab, Quaid-e-Azam Campus, Lahore 54590, Pakistan*
[3] *Centre of Excellence in Molecular Biology, University of the Punjab, Thokar Niaz Baig Lahore 53700, Pakistan*
[4] *Department of Botany, Kinnaird College for Women, Lahore 54000, Pakistan*
[5] *Institute of Physics Center for Science and Education, Silesian University of Technology, Krasińskiego 8A, Katowice 40-019, Poland*
[6] *PhD School, Silesian University of Technology, 44-100 Gliwice, Poland*
[7] *Centre for Applied Mathematics and Bioinformatics, Gulf University for Science and Technology, Hawally 32093, Kuwait*
[8] *Department of Chemistry, College of Science, King Khalid University, Abha 61413, Saudi Arabia*

Highlights

- These findings identify carboxyl and hydroxyl groups on f-MWCNTs as key contributors to boosting antifungal activity.
- Mycelial deformation and altered antioxidative activity demonstrated the multi-mechanistic antifungal action of f-MWCNTs.
- A notable drop in fungal bioactive metabolites showed that key fungal biochemical processes were disrupted, highlighting the novelty of this study.

Abstract

The study explores the antifungal properties of functionalized multi-walled carbon nanotubes (f-MWCNTs) against *Fusarium oxysporum* f. sp. *tuberos*i, revealing a concentration-dependent impact, with the lowest concentration suppressing mycelial development. The peaks at $2\theta°$=7.92° and 25.85° reveal the presence of MWCNTs. Furthermore, the bonding extremes at 3,194 and 2,441 cm^{-1} and the peak at 3,573 cm^{-1} are hydrogen-bonded. The peak at 3,756 cm^{-1} demonstrates the vibration of OH stretching to confirm the functionalization of MWCNTs. MWCNTs at 308 nm show a peak with much higher UV energy. This is because of the different plasmonic vibrations that the free electrons of multi-wall carbon nanotubes exhibit at about 308 nm. Scanning electron microscope (SEM) analysis revealed mycelial structure distortions, revealing inhibitory mechanisms of f-MWCNTs and their interaction with *F. oxysporum* f. sp. *tuberosi*, providing insights into their complex behavior. Multi-walled carbon nanotubes (MWCNTs) showed anti-oxidative properties, indicating potential multifaceted modes of action, as evidenced by 2′,7′-dichlorofluorescein diacetate dye testing. The current study analyzed bioactive molecules in *F. oxysporum* f. sp. *tuberosi* extracts by gas-chromatography-mass spectrometry (GC-MS) analysis, showing six metabolites having antimicrobial, cytotoxic, and antioxidant properties. However, exposure to f-MWCNTs reduced these potent molecule concentrations, highlighting the significant impact of f-MWCNTs on *F. oxysporum* f. sp. *tuberosi* biochemical arsenal. This is the first report that checked the antifungal, and antioxidant activity and of a lesser concentration of metabolites produced after the action of f-MWCNTs in *F. oxysporum* f. sp. *tuberosi*. This research highlights the potential of f-MWCNTs as antifungal agents, paving the way for innovative strategies in combating fungal pathogens and developing effective treatments.

Keywords: carbon nanotubes, antimicrobial activity, *Fusarium oxysporum* f. sp. *tuberosi*, Zeta potential, XRD, cell membrane

Received 6 February 2024; Received in revised form 20 March 2024; Accepted 28 April 2024; Available online 8 July 2024
Sadia Manzoor, E-mail: smnsnny@gmail.com; #Correspondence Muhammad Danish Ali, E-mail: muali@polsl.pl, Danishmsc15@gmail.com

© 2026 CAAS. Publishing services by Elsevier B.V. on behalf of KeAi Communications Co. Ltd. This is an open access article under the CC BY-NC-ND license (http://creativecommons.org/licenses/by-nc-nd/4.0/). Peer review under responsibility of Editorial Board of *Journal of Integrative Agriculture*.
doi: 10.1016/j.jia.2024.07.010

1. Introduction

Fusarium oxysporum f. sp. *tuberosi* is a pathogenic class of *Fusarium* species (Ramadan and Haleem 2023) that affects potato plants, causing a disease known as *Fusarium* wilt of potato. *Fusarium oxysporum* f. sp. *tuberosi* can cause significant losses in various other agricultural crops like tomatoes, melons, bananas, and cotton due to its diverse host range and vascular wilt disease inducing it (Hafiz *et al.* 2022; Kang *et al.* 2023; Liu *et al.* 2023). *Fusarium oxysporum* f. sp. *tuberosi* causes vascular wilt in plants resulting in leaf curling, vascular browning, progressive wilting, defoliation, stunting, and eventually, plant death (Shams *et al.* 2023). Fungi can produce secondary metabolites, which are extracellular compounds, which aid in decomposing various substrates and contain antimicrobial agents, contributing to their survival in the environment (Poleto *et al.* 2021; Zhang *et al.* 2023). Secondary metabolites (i.e., jasmonates, anthranilates, cyclic peptides, cyclic depsipeptides, xanthones, quinones, and terpenoids) of *F. oxysporum* f. sp. *tuberosi* have antimicrobial and antioxidant effects (Ibrahim *et al*. 2021). A number of researchers carried out investigations to investigate the adverse effects of *F. oxysporum* f. sp. *tuberosi* on the cultivation of potatoes (Ntemafack *et al.* 2023). To deal with the diseases that are caused by *F. oxysporum* f. sp. *tuberosi* in plants, a variety of strategies have been employed, including the use of both biocontrol agents (da Silva Santos *et al.* 2020) and chemical agents (Abdelwahab *et al.* 2023) to manage various isolates of *F. oxysporum* f. sp. *tuberosi*.

An integrated strategy is needed to increase plant tolerance to biotic and abiotic challenges and efficiently use resources to reduce plant diseases by increasing crop output. As a result, there is more interest in using nanoparticles to create nano-formulations that can replace traditional solutions with better effectiveness, less input, and lower environmental toxicity (Ashraf *et al.* 2021; Chen *et al.* 2022; Ahamad *et al.* 2023).

Nanotechnology is a multidisciplinary area concerned with materials and technologies at the nanoscale, which generally ranges from one to one hundred nanometers (Krithika *et al.* 2023). It includes a wide range of scientific disciplines and has several applications in agriculture, chemistry, physics, biology, medicine, engineering, and electronics (Saleemi *et al.* 2022). Because of their small size and high surface-to-volume ratios, nanoscale materials have unique characteristics. These characteristics make them useful for a wide range of applications, including biological and natural sciences (Thirugnanasambandan and Gopinath 2023). Nanoparticles are being studied for their ability to control plant diseases such as *Fusarium* wilt. Their distinct features make them ideal for pesticide delivery (Matras *et al.* 2022). Carbon nanotubes (CNTs) as a nanomaterial, exhibit exceptional physical, chemical, electrical, and mechanical properties (González-García *et al.* 2022). CNTs, nano-diamonds, fullerenes, carbon nano-onions, nanofibers, and other carbon-based nanomaterials have piqued the interest of academics and scientists in recent decades due to their outstanding physicochemical properties (Soffian *et al.* 2022). CNTs have tubular and concentric cylindrical structures produced by rolling graphene sheets (Stegarescu *et al.* 2022).

Multi-walled carbon nanotubes (MWCNTs) consisting of multilayer graphene sheets have drawn substantial attention based on their excellent physicochemical properties and found versatile uses across a wide range of sectors (Rahman *et al.* 2022). CNTs that are synthesized have limited potential due to their chemical inertness and amphiphobic nature (Tewari *et al.* 2023). This is due to the poor solubility and dispersibility characteristics of raw CNTs, causing self-aggregation and difficulty in dispersing solvents (Shoukat and Khan 2022). To effectively utilize CNTs unique properties, surface modification is needed to overcome these limitations and fully realize their full potential. Functionalization methods, including covalent and non-covalent approaches, have been studied for surface modification (Dubey *et al.* 2021). Acid oxidation is a commonly used method due to its simplicity and efficiency (Isgoren *et al.* 2023). It involves the chemical treatment of CNTs with oxidizing agents like potassium permanganate, nitric acid, sulfuric acid, hydrochloric acid, and hydrogen peroxide. This treatment enhances the solubility and reactivity of CNTs by introducing functional groups like carbonyl, hydroxyl, and carboxyl groups. This treatment has proven highly effective in improving the properties of CNTs (Maksimova *et al.* 2022). The antimicrobial potential is achieved by functionalization with various components resulting in efficient antimicrobial surfaces on MWCNTs (Ding *et al.* 2020). The surface of nanotubes containing covalently bonded functional groups or chemicals has a significant impact on microbial responses. CNT efficiency in antimicrobial applications is influenced by a variety of parameters, including their composition and surface characteristics such as length, size, number of graphene layers, and physical organization (dispersed or aggregated) (Tardast *et al.* 2023). Reactive oxygen species (ROS) are highly reactive molecules containing oxygen (superoxide radicals ($O_2^{-}\cdot$), hydroxyl radicals ($\cdot OH$), and hydrogen peroxide (H_2O_2)) (Abdullah *et al.* 2023) having a critical role in the signaling of cells and mechanisms belonging to defense. When ROS generated in excess induces oxidative stress as well as cellular components are damaged (Salem *et al.* 2022). Several mechanisms are involved in producing the reactive oxygen species (Bienert *et al.* 2007) when interaction takes place between MWCNTs and fungal cells by destroying fungal cell membranes, disrupting redox equilibrium, and activating oxidative stress pathways (Saleemi *et al.* 2022).

Factors influencing ROS generation include the physicochemical properties of nanoparticles, fungi species having varying cell wall composition and antioxidant defense mechanisms, and exposure time and concentration having an impact on the extent of ROS generation in fungal cells (Yu *et al.* 2020). Studies showed that MWCNTs have pro-inflammatory, pro-fibrotic, and pro-angiogenic effects. They also cause cytotoxic and oxidative stress, leading to the production of ROS and decreased cell viability, potentially triggering apoptosis (Ambreen *et al.* 2023).

CNTs have shown remarkable effectiveness in deactivating copper-resistant plant pathogenic microorganisms like *Ralstonia solanacearum* and *Fusarium graminearum*

(Wang *et al.* 2017). MWCNTs are being investigated for their antifungal properties against various fungi, including common pathogenic species. *Candida* spp., *Aspergillus* spp., *Cryptococcus* spp., *Trichophyton* spp., and *Fusarium* spp. are common pathogens that can cause infections in humans and plants (Gurunathan *et al.* 2022).

The bio-nanocomposites of MWCNTs generated showed antifungal activities against *Candida glabrata* and *Candida albicans*, with inhibition zones of 32 and 73%, respectively (Ibrahim *et al.* 2023). CNTs can improve agricultural sustainability by promoting plant growth, regulating nutrient and fertilizer release, and causing physiological changes, thereby boosting productivity in environmental stress conditions (Safdar *et al.* 2022).

MWCNTs may find applications in agriculture as antifungal agents for crop protection or as components of fungicidal formulations. Their controlled release in soil or on plant surfaces could help combat fungal infections in a targeted manner (Helal *et al.* 2022).

González-García *et al.* (2021) reported that MWCNTs controlled the *Alternaria solani* infecting the *Solanum lycopersicum* crops *via* ROS generation which subsequently reduced the infection of *Alternaria solani* and resulted in higher biomass and fruit output . Similarly, by improving photosynthetic activity and raising phytohormone production, 200 mg L^{-1} of CNT and fullerene given to *Nicotiana benthamiana* plants decreased the incidence and replication of the tobacco mosaic virus (González-García *et al.* 2022).

A substantial lessening in bacteria was achieved by adding the carboxyl group on MWCNTs, with results showing 30% for *Bacillus subtilis*, *Pseudomonas aeruginosa* with 27% along with 20–40% for *Escherichia coli*, and *Staphylococcus aureus* showing 15–50% inhibition (Mc Gee *et al.* 2020). *Vibrio parahaemolyticus*, *Escherichia coli*, *Staphylococcus aureus*, *Enterococcus faecalis*, *Lactobacillus acidophilus*, and *Bifidobacterium adolescentis* growth were inhibited by the carboxyl and hydroxyl functional group present on MWCNTS in a dose-dependent manner (Saleemi *et al.* 2022). *Staphylococcus aureus*, *Klebsiella pneumoniae*, *Pseudomonas aeruginosa*, and *C. albicans* are inhibited by non-covalently dispersed CNTs (double-walled carbon nanotubes, DWCNTs, and MWCNTs) (Saleemi *et al.* 2020). *Botrytis cinerea* on rose petals is efficiently inhibited by carbon nanomaterials and certain metal oxide nanoparticles at extremely low nanoparticle concentrations. Nanomaterials, therefore, combat fungus throughout the development of flowers (Ashraf *et al.* 2021). Multiwall CNTs functionalized with functional groups OH-, COOH-, and NH_2 against *Fusarium graminearum* exhibited strong antifungal activity. These MWCNTs might be used in plant protection because they prevent the growth and elongation of fungal spores (Thirugnanasambandan and Gopinath 2023).

The present study aimed to achieve the following objectives: (i) to characterize commercially obtained MWCNTs after acid functionalization using UV-Vis spectroscopy, fourier-transform infrared spectroscopy (FT-IR), scanning electron microscopy (SEM), and X-ray diffraction (XRD), thereby verifying structural and compositional modifications induced by functionalization; (ii) to evaluate the *in-vitro* antifungal activity of functionalized MWCNTs (f-MWCNTs) against *Fusarium oxysporum* f. sp. *tuberosi*, the causal agent of potato dry rot; (iii) to examine antimicrobial secondary active metabolites produced in fungal extract treated with f-MWCNTs and identify them using gas-chromatography-mass spectrometry (GC-MS); and (iv) to assess the antioxidant effects of f-MWCNTs on *F. oxysporum* f. sp. *tuberosi* by quantifying intracellular ROS using the fluorescent probe 2′,7′-dichlorodihydrofluorescein diacetate (DCFH-DA), thereby elucidating the physiological and virulence-related impacts of carbon nanomaterials on this phytopathogen.

2. Materials and methods

2.1. Various parameters of MWCNTs

MWCNTs were purchased from Hongwu International Group Ltd. (Xuzhou, Jiangsu, China) for the proposed study. These MWCNTs exhibit a high purity of greater than 95% by weight. The outer diameter (OD) of the nanotubes ranges from less than 10 to 20 nm, and their length varies from 30 to 100 μm. The specific surface area (SSA) is greater than 200 m^2 g^{-1}, and the ash content is less than 2.0% by weight. The ignition temperature of these nanotubes exceeds 611°C, and they have an electrical conductivity (EC) greater than 100 S cm^{-1}. The nanotubes are black in color, with a tap density of 0.07 g cm^{-3}. These MWCNTs were synthesized using the chemical vapor deposition (CVD) method.

2.2. Microscopic features of *F. oxysporum* f. sp. *tuberosi* analysis

The *F. oxysporum* f. sp. *tuberosi* (accession no. FCBP-SF-606) was provided by the Faculty of Agriculture Sciences, University of Punjab, Lahore, Pakistan. Fungi responsible for potato diseases were carefully revived and purified for use in the study. For the microscopic characterization of mycelial and spore characteristics, parameters (colony shape, growth behavior, pigmentation, hyphal structure, septation, branching, macroconidia, microconidia, and chlamydospores), and micrometry were used. These characteristics were defined using the procedures described by (Akram *et al.* 2014). A morphological approach by using a scanning electron microscope with STEM analysis was also used to identify *F. oxysporum* f. sp. *tuberosi* specific structure.

2.3. Functionalization of MWCNTS

Functionalizing MWCNTs is a process aimed at incorporating acid groups onto their surface, thereby enhancing their dispersibility in solvents and compatibility with other materials. Prepared the acid mixture by combining 80 mL of 15.8 mL HNO_3 with 18.4 mL of concentrated H_2SO_4, maintaining a ratio of HNO_3 to H_2SO_4 at 1:3 (v/v). Added the 0.3 g MWCNTs into the acid mixture, ensuring their uniform dispersion by vigorous stirring and employing ultra-sonication at a temperature of 40°C. Allowed the reaction to proceed for 2.5 h. Upon completion, the functionalized MWCNTs were separated from the acid by vacuum filtration through a 3 μm porosity filter paper. Thoroughly wash the functionalized

MWCNTs with deionized water multiple times until the pH 7 becomes the same as that of deionized water to eliminate any residual acid. Subsequently, the functionalized MWCNTs dried under vacuum conditions at 100°C for 8 hours. This critical step is essential for removing any remaining water and ensuring the stability of the functionalized MWCNTs (Jun *et al.* 2018).

2.4. Characterization of CNTs

The characterization of CNTs is done by using different techniques.

UV-vis spectrum UV-vis spectrum of CNTs was performed with a range of 600 nanometers by using a spectrophotometer (V-780 UV-visible/Near Infrared Spectrophotometer, JASCO Inc., Japan). The study used ultrasonography to disperse MWCNTs in an aqueous solution containing 1% Tween 80 for 40 min, with ice water added to prevent temperature elevation. The stability of MWCNTs at different concentrations (150–550 μg mL^{-1}) was assessed, and dispersibility was evaluated using a UV spectrophotometer. CNTs typically show significant absorption in the UV region and a distinctive peak in the visible range, typically between 400 and 700 nm.

XRD XRD is used to check the state of nanoparticles either amorphous or crystalline and includes scanning of powder sample 2θ at the current 40 mA with a range of 5 to 40º by using a Diffractometer (Bruker AXS, Karlsruhe, Germany), using Cu-Kα radiation and a diffracted beam monochromator. The multi-walled carbon nanotube solution was cast onto a glass substrate and air-dried under ambient conditions to prepare samples for measurements.

FTIR-spectrum FTIR-spectrum applied to ascertain the nature of the functional group and type in CNTs after purification by using Agilent Cary 630 FTIR System, Agilent Technologies, USA, with a scan range of 400 to 4,000 cm^{-1}.

SEM SEM is employed to investigate the morphology of nanoparticles. A 10 mg dry powder of MWCNTs sample was used to create SEM micrographs using an aluminum stub, and a carbon pasted disc by using a scanning electron microscope (Nova Nano SEM 450, FEI Co., Hillsboro, OR, USA).

In vitro* antifungal activity of MWCNTs against *F. oxysporum* f. sp. *tuberosi To get the final working concentration solution of CNTs (150–550 μg mL^{-1}), CNTs were dissolved in 1% Tween 80 in deionized water. Before adding media to 85 mm disposable Petri dishes, 100 μL of levofloxacin (250 mg/50 mL ddH_2O), an antibacterial solution, was placed into the 100 mL of PDA growth medium prior to pouring. Calculations were used to determine the minimal inhibitory concentration (MIC) for various CNT concentrations. Different growth parameters of *F. oxysporum* f. sp. *tuberosi* such as growth pattern, mycelial pigmentation, and colony diameter, were observed, compared with uninoculated *F. oxysporum* f. sp. *tuberosi*, which is the control plate, and the gathered data was statistically evaluated. Statistics were applied to all the data. The minimum inhibitory concentration of mycelial growth is determined using the following formula (Yassin *et al.* 2022).

$$\text{Percentage of inhibition (\%)} = \frac{C-T\times 100}{C} \quad (1)$$

where C represents the mean diameter of the fungal colony (in cm) on the positive control and T represents the average diameter of the fungal colony (in cm) on the treatment plates.

Antioxidant activity and ROS generation To monitor reactive oxygen species creation and cell survival, an effect on the membrane in *F. oxysporum* f. sp. *tuberosi* produced by CNTs was observed using DCFH-DA (Sigma-Aldrich, St. Louis, MO, USA) with little modification in the method used by Ashraf *et al.* (2021). *F. oxysporum* f. sp. *tuberosi* mycelial discs cut from the untreated and treated sample with concentration (550 μg mL^{-1} of MWCNTs) were taken from the periphery of a 7-day-old culture and suspended in PBS. After centrifugation, re-rinsed with sterile PBS and treated with 5 μmol L^{-1} of the fluorescent dye DCFH-DA (Sigma-Aldrich) for 30 min at room temperature in the absence of light. After DCFH-DA treatment, samples were washed three times to remove excess dye.

Additionally, fluorescence observation with an inverted fluorescent microscope (DM, Leica Germany) was employed to identify the buildup of ROS in the hyphae using DCFH-DA dye. The intensity of the fluorescence was measured through a spectrophotometer (V-780 UV-visible/Near Infrared Spectrophotometer) with excitation at 492 nm and emission at 517 nm (Ashraf *et al.* 2021).

2.5. GC-MS technology

GC-MS technology was employed to identify the mycotoxin produced through the interaction of CNTs with *F. oxysporum* f. sp. *tuberosi*. Agilent Technologies Inc. (Agilent Technologies, Wilmington, DE, USA) provided the instrumentation for the GC-MS experiments, utilizing the GC 7890 B and MS 5977 C systems. The injection system maintained a constant temperature of 275°C, with samples injected using an auto-sampler. Helium gas was used as the carrier at a flow rate of 1 mL min^{-1}, while the oven temperature was set to 300°C with an auxiliary temperature of 280°C.

Different ramp time specifications were utilized for the GC 7890 B and MS 5977 C systems, with varying rates and temperatures for each step. A column with a different diameter was employed to separate chemicals, utilizing a nonpolar phenyl arylene polymer similar to (5%-phenyl)-methylpolysiloxane, which provided an excellent signal-to-noise ratio for analytical purposes.

The mass hunter software package from the NIST 17.L collection was used to analyze the metabolites. Subsequently, molecules identified through the NIST 17.L library were cross-referenced with the PubChem online database to determine their corresponding molecular mass and formula (Thamer and Thamer 2023).

3. Results

3.1. Microscopic and morphological characterization of *F. oxysporum* f. sp. *tuberosi*

The vegetative and reproductive features of *F. oxysporum* f. sp. *tuberosi* were characterized by using a light microscope (LABOMED C x L, USA). The morphology of the potato

vascular wilt pathogen appeared as white to purple, with pigmentation along with smooth and heavy spreading, septate, homogeneous mycelia, and a cottony and fluffy appearance (Fig. 1). Microconidia (oval or kidney-shaped), Monophialides, and chlamydospores are structures on which they were observed in the microscope growing radially within 5 to 7 days (Fig. 2). The structure of *F. oxysporum* f. sp. *tuberosi* was also analyzed by using a scanning electron microscope with STEM analysis, showing that the mycelium of *F. oxysporum* f. sp. *tuberosi* is polydisperse, oval, and spherical-shaped (Fig. 3).

3.2. Characterizations of MWCNTs

UV/Vis, FT-IR, SEM, and XRD were used in this investigation to validate the characteristics of f-MWCNT. The following techniques were used to characterize commercially synthesized CNTs after acid functionalization.

UV-visible spectroscopy The UV-visible absorption spectra of f-MWCNTs were measured with a UV-spectroscopy V-780 UV-visible/near infrared spectrophotometer. At a wavelength of 600 nm, absorbance measurements were taken. Individual CNTs with varied diameters exhibit unique properties in the UV light spectrum, with longer wavelengths correlating to lower amplitudes. Notably, as seen in Fig. 4-A accompanying the graph, functionalized MWCNTs have conspicuous UV peaks centered at around 308 nm due to unique plasmonic vibrations of free electrons in nanotubes at roughly 308 nm. The strength of these peaks can be attributed to the CNTs

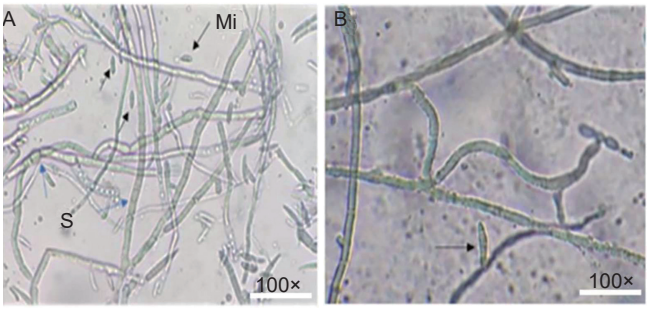


Fig. 2 Microscopic observations of hyphae of *Fusarium oxysporum* f. sp. *tuberosi*. In A, Mi, microconidia shown with black arrows; S, septa with blue arrows. In B, black arrow shows macroconidium.

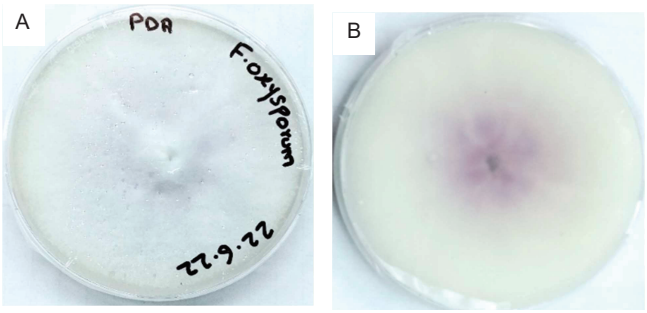


Fig. 1 The plate of *Fusarium oxysporum* f. sp. *tuberosi*. A, front view. B, backward view with purple pigmentation.

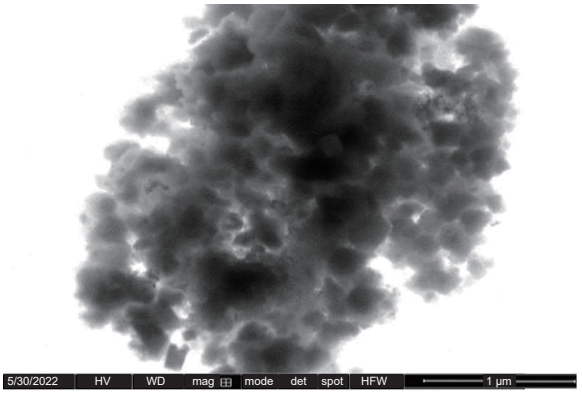


Fig. 3 SEM using STEM detector micrograph of *Fusarium oxysporum* f. sp. *tuberosi*.

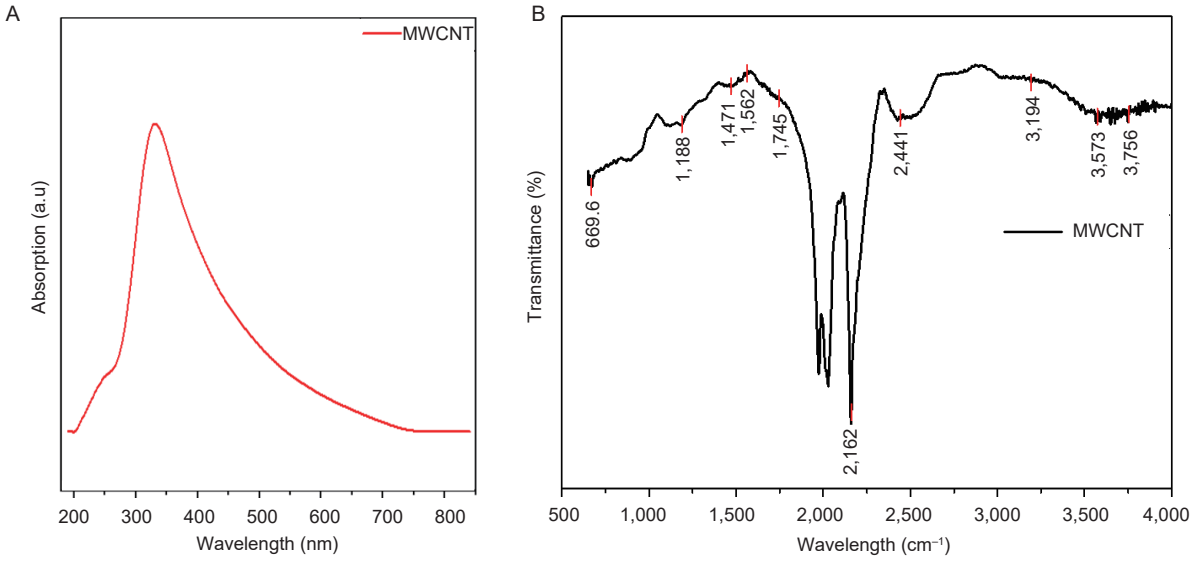


Fig. 4 UV-visible (A) and FT-IR (B) spectrum of multi-walled carbon nanotubes (MWCNTs).

unusually narrow size distribution, which may be due to almost uniform tube lengths and widths (Saleemi and Lim 2022).

FT-IR FT-IR spectroscopy was used to examine the spectral properties of MWCNTs in the 400–4,000 cm^{-1} range, revealing unique wave numbers. Fig. 4-B depicts the FT-IR spectra of f-MWCNTs, with strong peaks at 3,194 and 2,441 cm^{-1}. Notably, the peak at 3,573 cm^{-1} shows the presence of hydrogen bonds, whereas the peak at 3,756 cm^{-1} corresponds to the vibration associated with OH stretching. Furthermore, peaks seen at 1,745 and 1,562 cm^{-1} may be attributable to the vibrational modes of stretched ester (C=O) bonds. The identification of hydroxyl and carboxyl functional groups is supported by FTIR spectroscopy (Santos *et al.* 2019).

XRD X-ray diffraction was used in the study to examine the structural characteristics of f-MWCNT. As shown in Fig. 5, the XRD spectra of the f-MWCNT samples displayed different diffraction peaks at two particular angles, 2θ°=7.92° and 25.85°. These peaks provide critical information on the crystallographic nature of f-MWCNTs. The most significant diffraction peak at 25.85° is very notable. This peak corresponds to the typical graphitic peak, which is due to the tubular arrangement of carbon atoms within f-MWCNTs. The tubular structure of f-MWCNTs, which is made up of nested carbon nanotubes, causes hexagonal graphite-like layers to develop. The prominent diffraction peak at 2θ°=25.85° is identified as the (0 0 2) reflection of this hexagonal graphite structure (Rahman *et al.* 2022).

SEM SEM investigation offers decisive insights into the morphological attributes of f-MWCNTs, serving as a valued foundation for understanding their properties. The distinctive form of the f-MWCNTs after SEM examination is shown in Fig. 6. f-MWCNTs were found with well-aligned structures and consistent thickness with a diameter of 18.5 nm along with 100 μm length. Furthermore, SEM imaging allowed the identification of other intriguing features in the morphology of carbon nanomaterials, most notably the presence of spherical and tubular nanoparticles as described in previous studies (Sanukrishna and Jose 2022), which exhibited diverse shapes, contributing to the overall structural complexity.

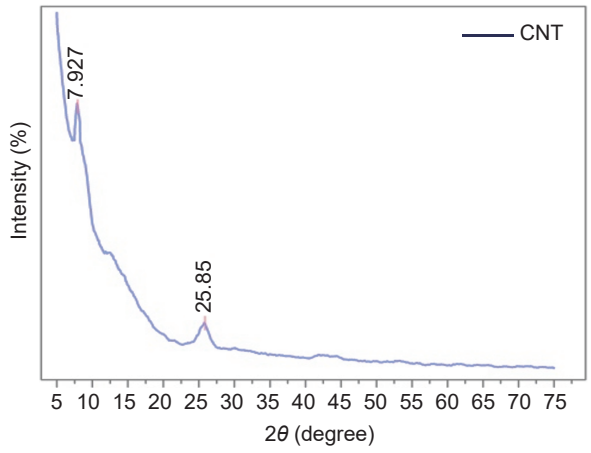


Fig. 5 XRD patterns of multi-walled carbon nanotube (MWCNT).

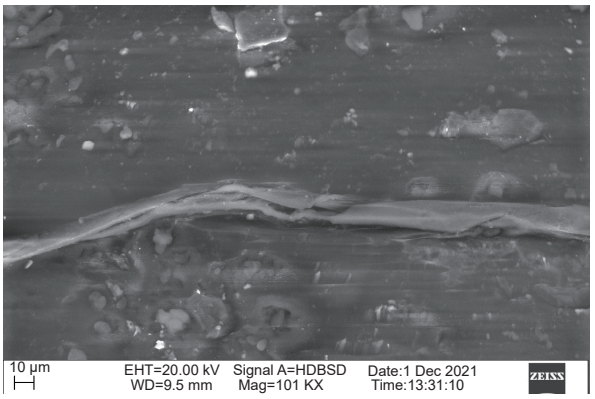


Fig. 6 SEM micrograph of f-multiwalled carbon nanotubes.

Antifungal activity of f-MWCNTs against *F. oxysporum* f. sp. *tuberosi* *In-vitro* studies were conducted on CNTs to determine their antimicrobial activity toward *Fusarium*. Comparing the *in-vitro* results to the control, they were notable. Functionalized MWCNTs affected the *F. oxysporum* f. sp. *tuberosi* hyphae density, suggesting that carbon-based nanomaterials had an impact on the organism's biomass. When the concentration of carbon-based nanomaterials increases, notably f-MWCNTs, could significantly lower *F. oxysporum* f. sp. *tuberosi* biomass, and the biomass of the hyphae of *F. oxysporum* f. sp. *tuberosi* decreased. f-MWCNTs's capacity to prevent fungal hyphae from branching further accounts for their ability to effectively reduce the mycelial biomass of *F. oxysporum* f. sp. *tuberosi*.

Fig. 7 showed that f-MWCNTs significantly (P<0.05) lowered and suppressed the biomass of *F. oxysporum* f. sp. *tuberosi* in a dose-dependent manner. In comparison to the untreated control, the greatest percentage of *F. oxysporum* f. sp. *tuberosi's* mycelial radial growth suppression was determined to be 93.2% at 550 μg mL^{-1}. At 150 and 250 μg mL^{-1} of f-MWCNTs, the inhibition rate decreased by 50% (14.4 and 29.3, respectively) (Fig. 5). The presence of higher concentrations of f-MWCNTs significantly decreased fungal biomass, while spore development was inhibited at levels reaching 450 μg mL^{-1} (Table 1), which resulted in a reduction of 77.9%, compared to none for the control. The highest fungal growth suppression was seen at 550 μg mL^{-1}, or 93.2% (Wang *et al.* 2017; González-García *et al.* 2021). Similar efficacy to that of nanoparticles as reported by Alexandru *et al.* (2020), Siddiqui *et al.* (2020), and Farhana *et al.* (2022) revealed considerable fungal suppression using CNT nanoparticles.

Unlike the standard growth pattern observed in the control, the development of *F. oxysporum* f. sp. *tuberosi* was notably delayed when exposed to different concentrations (150–550 μg mL^{-1}) of f-MWCNTs, taking over two weeks to complete growth in a Petri plate (Fig. 8). One to three septate macroconidia, solitary conidia, and many chlamydospore chains with an average diameter of 5 to 10 m may be observed during examination. Multiseptated, properly branched, light yellow-pigmented, spongy hyphal cells may also be observed (Ajmal *et al.* 2022).

Antioxidant activity and investigation of ROS production

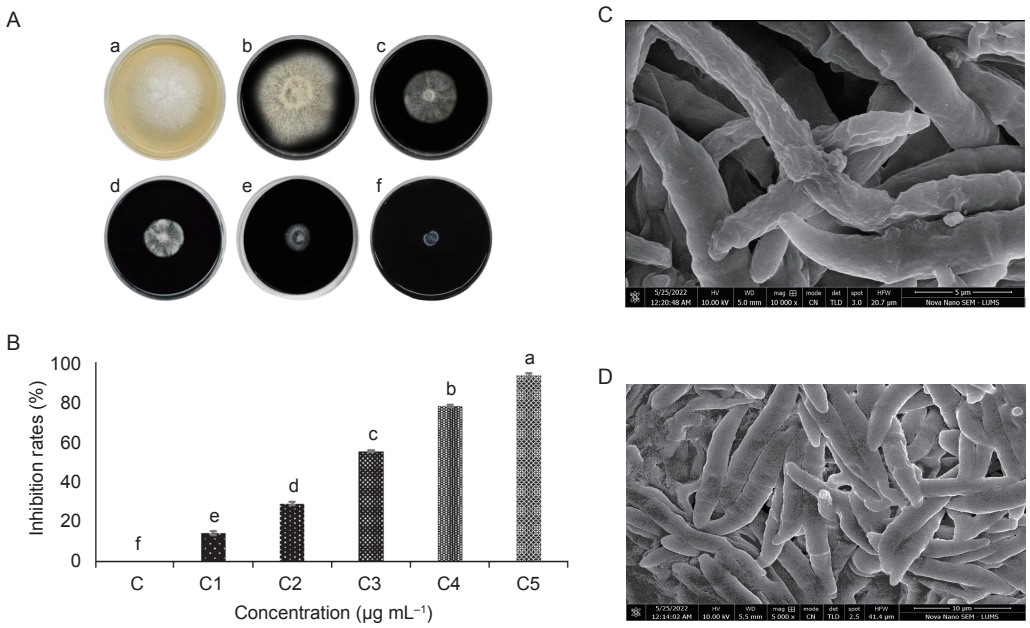


Fig. 7 Biomass of *Fusarium oxysporum* f. sp. *tuberosi*. A, *F. oxysporum* f. sp. *tuberosi* treated with different concentrations of f-multi-walled carbon nanotubes (f-MWCNTs). a–e, 150, 250, 350, 450, and 550 μg mL^{-1}. f, uninoculated control. B, % growth inhibition of treated *F. oxysporum* f. sp. *tuberosi* with f-MWCTs in comparison to control (non-treated *F. oxysporum* f. sp. *tuberosi*). C–C5, 150, 250, 350, 450, and 550 μg mL^{-1}. All plates were incubated at (27±1)°C for 7 days. C and D, SEM micrograph of untreated *F. oxysporum* f. sp. *tuberosi* (C) and treated *F. oxysporum* f. sp. *tuberosi* with f-MWCNT (550 μg mL^{-1}) (D). The bar represents ±standard error of the mean (n=3). Tukey's multiple comparison test results reported with a significance level of P<0.05.

Table 1 F-multiwalled carbon nanotubes (f-MWCNTs) treated *Fusarium oxysporum* f. sp. *tuberosi* growth inhibition (%)

Concentration (μg mL^{-1})	MWCNTs (% inhibition)
150	14.4 e
250	29.3 d
350	55.3 c
450	77.9 b
550	93.2 a
Untreated *F. oxysporum*	0.0 f

The bar represents ±standard error of the mean (n=3). Tukey's multiple comparison test results reported with a significance level of P<0.05.

Negatively charged nanoparticles and pathogens are electrostatically attracted to one another. When microbes encounter nanoparticles, light energy causes ROS to be created at the microbial surface. Nanoparticles then induce toxicity, leading to oxidative stress and the release of cytochrome c in the mitochondria, which triggers cell death. Fluorescence microphotographs of the *F. oxysporum* f. sp. *tuberosi* treated with f-MWCNT nanoparticles (at 150–550 μg mL^{-1}) and control (untreated) as shown in Fig. 8. To detect intracellular ROS development in fungal mycelium, DCFH-DA fluorescence was used. In contrast to the control (untreated) sample, mycelial samples treated with f-MWCNT showed an increase in the expression of fluorescence (Fig. 9-A, B–F). The study found a dose-dependent increase in reactive oxygen species (ROS) levels in fungi treated with f-MWCNTs. The ROS generation varied at different concentrations and was determined relative to untreated *Fusarium* control (100%), with a peak of (260±11.2)%, (350±14.3)%, (405±7.24)%, (512±12.76)%, and (607±8.40)% at 150, 250, 350, 450,

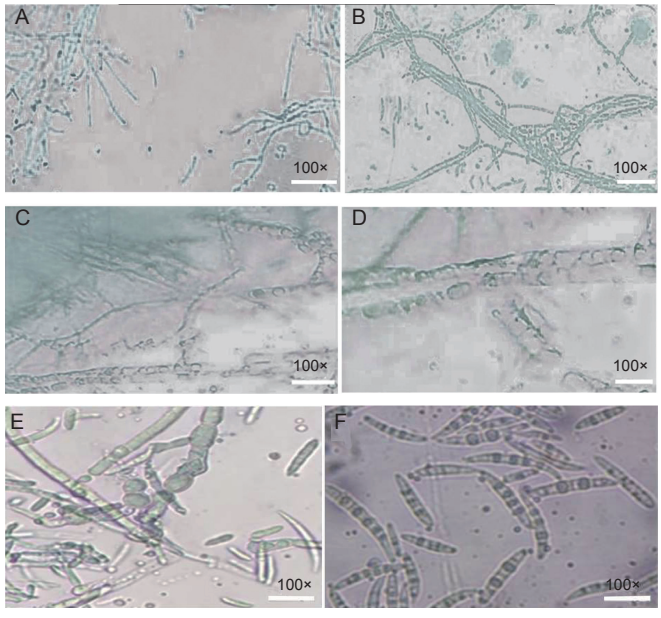


Fig. 8 *Fusarium oxysporum* f. sp. *tuberosi* hyphae. A, untreated. B–F, observation by light microscope after 150–550 μg mL^{-1} treatments with f-multiwalled carbon nanotubes (f-MWCNTs), deformed hyphae after treatment with f-MWCNTs changed into a chain of chlamydospore. F, macroconidia showing 3–5 sickle-shaped septum and microconidia.

and 550 μg mL^{-1} of f-MWCNTs, respectively (Azizi-Lalabadi *et al.* 2020). *Fusarium oxysporum* f. sp. *tuberosi* samples treated with f-MWCNTs also showed increased fluorescence intensity, which intensified with increasing concentrations.

The fluorescence intensity was directly proportional to the quantity of reactive oxygen species in the sample, a relationship quantified and correlated with ROS production, as illustrated in Fig. 10.

Hence, the increased ROS in *F. oxysporum* f. sp. *tuberosi* following exposure to f-MWCNTs interacts with several pathways in the filamentous fungus, which may be the main reason for the inhibition of mycelial development and death (Azizi-Lalabadi *et al.* 2020; Ding *et al.* 2020). Overall, the effects of f-MWCNTs on *Fusarium* and the use of DCFH-DA fluorescence to identify intracellular ROS formation in fungal mycelium led to the finding that f-MWCNTs cause pathogen cell membrane breakdown by creating ROS. These findings align with studies conducted by multiple scientists on microorganisms (Pariona *et al.* 2019; Saleemi and Lim 2022).

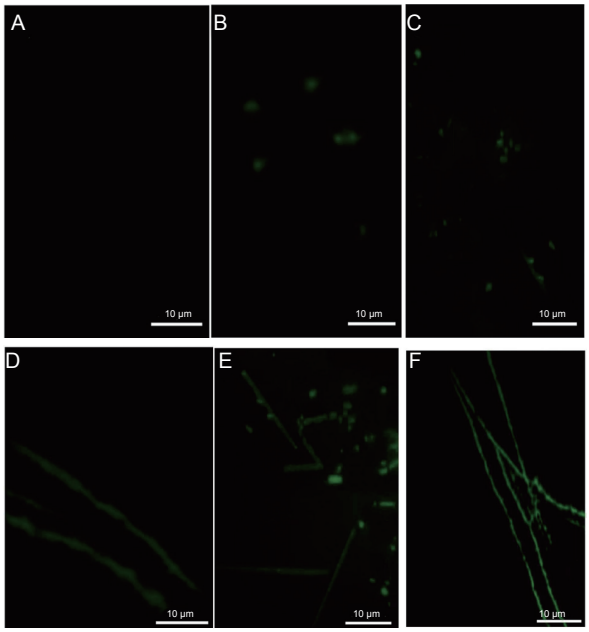


Fig. 9 Reactive oxygen species (ROS) buildup is visualized by fluorescence microscopy. A, uninoculated *Fusarium oxysporum* f. sp. *tuberosi*. B–F, the hyphal cells of *F. oxysporum* f. sp. *tuberosi* inoculated with 150–550 μg mL^{-1} f-multiwalled carbon nanotubes (f-MWCNTs) nanoparticles by applying DCFH-DA dye.

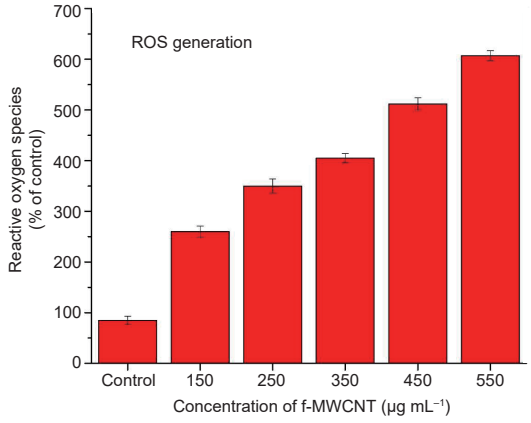


Fig. 10 Reactive oxygen species (ROS) generation. The intensity of green fluorescence was measured using DCFH-DA assay (exposure of *Fusarium oxysporum* f. sp. *tuberosi* hyphae against 150, 250, 350, 450, and 550 μg mL^{-1} concentrations of f-multiwalled carbon nanotubes (f-MWCNTs)). Control, untreated hyphae. The bar represents ±standard error of the mean (n=3). Tukey's multiple ranges test results reported with a significance level of P<0.05.

GC-MS-analysis GC-MS study, indicating the existence of forty-four bioactive chemicals in *F. oxysporum* f. sp. *tuberosi* extracts grown in a medium containing f-MWCNTs as represented in Fig. 11. Among them only six metabolites were identified from chromatograph having antimicrobial metabolites, as shown in Fig. 12-A–F), the analysis revealed the existence of these chemicals with consistent peaks at varied retention durations. Table 2 shows the chemicals that have been identified. Earlier research demonstrated that catechol and its derivatives possess cytotoxic properties. Malekinejad *et al.* (2023) content was determined to be 6.36% in this GC-MS study as shown in Fig. 12-A. Furthermore, at 6.15%, methoxy-4-vinyl phenol (2M4VP) was discovered (Nandhini *et al.* 2021), a phenolic molecule found in *F. oxysporum* f. sp. *tuberosi* extract-treated f-MWCNTs that has been shown in previous research to have anti-inflammatory activities. 2-Pyrrolidinone, a metabolite detected in the chromatograph at 4.47% concentration as shown in Fig. 12-B, was also reported in the previous study (Rees *et al.* 2007). Moreover, functional n-hexanoic acid as shown in Fig. 12-C, a metabolite found at 1.23%, was identified, correlating with previous studies, and confirming its potential as an antibacterial agent (Rosengaus *et al.* 2004). Canolol, also known as 4-vinyl-2,6-dimethoxyphenol, was found at 0.69% as represented in Fig. 12-D. It was extracted from *F. oxysporum* f. sp. *tuberosi* extracts treated with f-MWCNTs, confirming prior studies highlighting its effects on oxidative stress and mutagenesis (Galano *et al.* 2011). Another investigation discovered that orcinol is a secondary metabolite found in Lepraria species (Nelsen and Gargas 2008). It was also discovered in the *F. oxysporum* f. sp. *tuberosi* extract in the current investigation, accounting for 0.55% of the content Fig. 12-F.

4. Discussion

Fusarium oxysporum f. sp. *tuberosi*, a soilborne fungal pathogen, is a major threat to potato crops, causing vascular wilt and root rot diseases (Yu *et al.* 2022; Ekwomadu and Mwanza 2023).

Fusarium oxysporum f. sp. *tuberosi* is a fungal pathogen with a white to pale pink mycelium and cottony texture. It forms hyphae, conidia, chlamydospores, microconidia, and sclerotia. It causes vascular wilt in potato plants and reproduces asexually or sexually (Wale *et al.* 2008; Li *et al.* 2022).

Conventional methods like chemical herbicides and traditional fertilizers have constraints because of environmental concerns and the emergence of resistance (Abdelwahab *et al.* 2023). Nanotechnology, on the other hand, offers long-term and effective solutions (Yadav *et al.* 2023). Carbon-based nanomaterials, notably CNTs, have attracted interest due to their extraordinary physiochemical

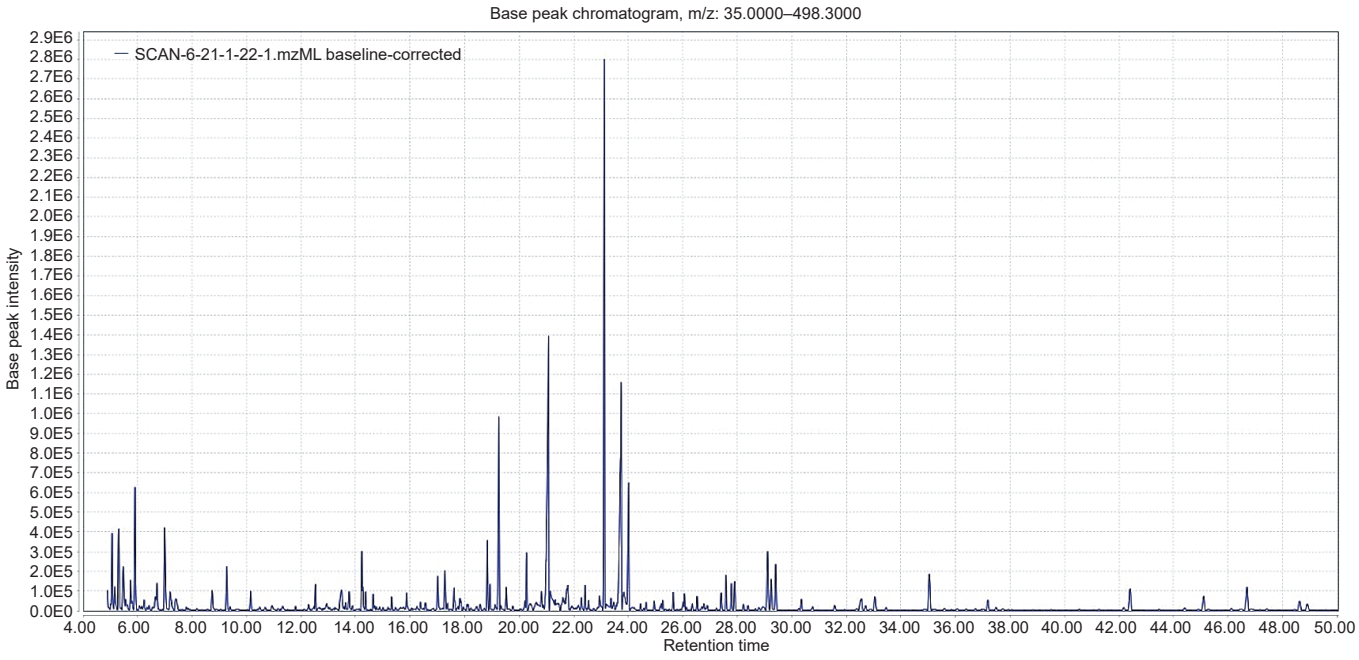


Fig. 11 Gas chromatogram showing 44 main peaks in *Fusarium oxysporum* f. sp. *tuberosi* treated with f-MWCNTs.

Table 2 Compounds identified from f-multiwalled carbon nanotubes (f-MWCNTs) treated *F. oxysporum* f. sp. *tuberosi* through GC/MS analysis

Serial no.	Compound name	Molecular formula	Molecular weight (g mol^{-1})	Retention time (min)	% of total	References
1	Catechol	$C_6H_6O_2$	110.11	6.743	6.36	Malekinejad *et al*. (2023)
2	2-Methoxy-4-vinyl phenol	$C_9H_{10}O_2$	150.17	9.283	6.15	Nandhini *et al*. (2021)
3	2-Pyrrolidinone	C_4H_7NO	85.1	5.197	4.47	Rees *et al*. (2007)
4	n-Hexadecanoic acid	$C_{16}H_{32}O_2$	256.42	20.820	1.23	Rosengaus *et al*. (2004)
5	2,6-Dimethoxy-4-vinyl phenol	$C_{10}H_{12}O_3$	180.20	14.236	0.69	Galano *et al*. (2011)
6	Orcinol, 2TMS derivatives	$C_{13}H_{24}O_2Si_2$	268.5	11.819	0.55	Nelsen and Gargas (2008)

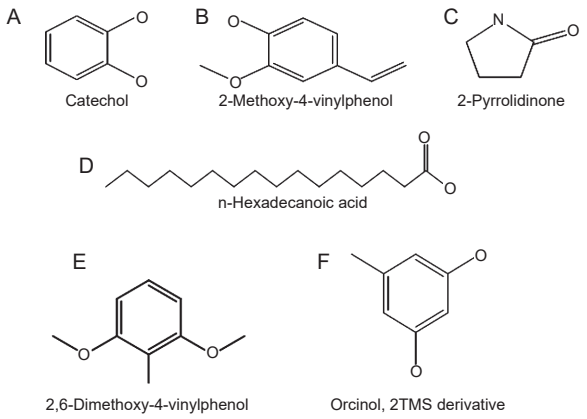


Fig. 12 A secondary metabolite found in the *Fusarium oxysporum* f. sp. *tuberosi* extract treated with f-multiwalled carbon nanotubes (f-MWCNTs). The detected metabolites were cathocol (A), 2-methoxy-4-vinyl phenol (B), 2-pyrrolidinone (C), n-hexadecanoic acid (D), 2,6-dimethoxy-4-vinylphenol (E), and orcinol, 2 Tms derivative (F).

properties, such as their small size, large surface area, and ability to penetrate cell membranes. Nonetheless, CNTs can be harmful, reducing cell viability and triggering apoptosis. Their potential influence on microbial diversity and beneficial microorganism viability has also been investigated (Safdar *et al.* 2022).

This research focuses on the characterization of f-MWCNTs, intending to define their stability and favorable functional groups that preserve a stable crystalline structure. UV spectroscopy is a useful analytical instrument that provides information on purity, concentration, and alterations. The discovery of a UV absorption peak in MWCNTs at 308 nm is an important result that sheds light on their electrical characteristics and plasmonic activity and our results are in accordance with the previous report (Saleemi *et al.* 2020).

XRD research revealed a typical signal for MWCNTs at 25.85°, highlighting their exceptional purity and crystalline structure. This discovery is consistent with previous CNT study (Rahman *et al.* 2022).

SEM analysis provides insights into the physical attributes and morphological features of f-MWCNTs, revealing a specific diameter of 18.5 nm and length 100 μm profile, individual unaggregated elongated tube, and the absence of impurities in the samples (Khalid *et al.* 2022; Sanukrishna and Jose 2022).

In this study, FTIR spectra and SEM images were used to examine structural changes in MWCNTs after functionalization. Stretching vibrations in MWCNTs were revealed by the FTIR spectra, which included unique peaks at 1,745, 1,562, 3,194, 2,441, 3,756, 3,573, and 3,573 cm^{-1}. The presence of numerous functional groups on the surface of f-MWCNTs confirms prior studies on CNT functionalization. Notably, the presence of carboxylic acid and hydroxyl groups corresponds to the findings of Sarode *et al.* (2023) and Sun *et al.* (2002). Furthermore, the discovery of hydrogen-bonded functional groups is consistent with findings from another research (Santos *et al.* 2019). In conclusion, the FTIR spectra and SEM analysis provide evidence of the existence of oxygen-containing functional groups as well as show MWCNTs being transformed from agglomerated structures to unbundled structures with decreased length after functionalization.

This study investigated the *in-vitro* antifungal capabilities of f-MWCNTs and their disruptive effect on *F. oxysporum* f. sp. *tuberosi*, providing insights for possible uses in agriculture and fungal disease management. SEM was used to analyze the mechanism of action of f-MWCNT on *F. oxysporum* f. sp. *tuberosi* and discovered that f-MWCNT inhibits *F. oxysporum* f. sp. *tuberosi* growth by generating distortions in fungal hyphae and aberrant morphological alterations. This gives a thorough explanation of the antifungal effects, which are also supported by prior research (Wang *et al.* 2017; González-García *et al.* 2021) proposed that the generation of reactive oxygen species (ROS) might be a critical element in suppressing fungal development, which was also investigated in our investigation since f-MWCNTs were discovered to produce ROS accumulation, leading to modifications in their cell walls. Scanning electron microscopy and dichloro-dihydro-fluorescein diacetate staining were used to evaluate these results. Farhana *et al.* (2022), Alexandru *et al.* (2020), and Siddiqui *et al*. (2020) found comparable efficacy to nanoparticles, indicating significant fungal suppression by the use of CNT nanoparticles (Alexandru *et al.* 2020; Siddiqui *et al.* 2020; Farhana *et al.* 2022).

There is an interrelated relationship between growth inhibition and the intensity of secondary metabolism in biological systems. Secondary metabolic changes are frequently used as adaptive responses (Kovač *et al.* 2020a). Our current study investigates the antifungal capabilities of MWCNTs on *F. oxysporum* f. sp. *tuberosi* as well as their impact on secondary metabolism. We further investigated the antioxidant activity of f-MWCMTs by assessing the generation of antimicrobial metabolites and identified six compounds using gas-chromatography spectrometry. The results from GCMS analysis confirm a reduction in the concentration of cathocol by 6.36%, 2-methoxy-4-vinyl phenol by 6.15%, 2-pyrrolidinone by 4.47%, n-hexadecanoic acid by 1.23%, 2,6-dimethoxy-4-vinylphenol by 0.69%, and orcinol, 2Tms derivative by 0.55%, all of which are indicative of modulation in fungal secondary metabolism, as previously reported in various studies. In summary, our findings align with prior research on the impact of fuller nanoparticles on the biomass production of mycotoxigenic fungi and the modulation of secondary metabolites (Kovač *et al.* 2020b).

5. Conclusion

Finally, our *in-vitro* study on the antifungal properties of f-MWCNTs revealed a concentration-dependent effect. Notably, at the lowest concentration of 550 μg mL^{-1}, there was a significant suppression of *F. oxysporum* f. sp. *tuberosi* mycelial growth. SEM analysis has revealed insights into the apparent distortion found in mycelia, which may explain mycelial growth inhibition. The findings suggested that f-MWCNTs may initiate cellular degradation and prompt oxidative stress-mediated apoptotic death in fungi. Notably, similar findings also apply to f-MWCNTs, which have been shown to exhibit antioxidative characteristics by DCFH-DA dye testing. Furthermore, we discovered 44 bioactive molecules in *F. oxysporum* f. sp. *tuberosi* extracts, with only six of these metabolites demonstrating antimicrobial capabilities, and their concentrations significantly reduced after exposure to f-MWCNTs. These findings highlight the potential of f-MWCNTs as powerful antifungal drugs and provide important insights into their mode of action on *F. oxysporum* f. sp. *tuberosi*.

6. Future prospects

The study explores the use of CNTs to effectively manage *F. oxysporum* f. sp. *tuberosi*, a potent phytopathogen, paving the way for eco-friendly agriculture strategies. Understanding signaling pathways will enhance our knowledge and enable targeted strategies for managing fungal diseases in agriculture, contributing to sustainable and environmentally friendly solutions. Research on the effects of nanoparticles on oxidative status evaluation on secondary metabolite by focusing on gene expression should continue.

Acknowledgements

The authors extend their appreciation to the Deanship of Scientific Research at King Khalid University, Saudi Arabia, for funding this work through a research group under grant number R.G.P-2/102/45. We are grateful to the Silesian University of Technology, Poland, and the University of the Punjab, Lahore, Pakistan for their support of research activities.

Declaration of competing interest

The authors declare that they have no conflict of interest.

Declaration of generative AI and AI-assisted technologies in the writing process

The authors declare that they did not use AI in the preparation and writing of this manuscript.

References

Abdelwahab N, Rabie W, Mohamed F. 2023. Fabrication and characterization of novel biocomposite based on Sargassum vulgare for controlling sugar beet root diseases. *Chemical and Biological Technologies in Agriculture*, **10**, 52.

Abdullah H, Sazeli S, Mamat N, Hapidin H, Sulong S. 2023. ROS Modulate cell death mechanism in cervical cancer cells treated with the combination of polyphenolic compounds and anticancer drug cisplatin: A review. *Current Cancer Therapy Reviews*, **19**, 334–348.

Ahamad L, Azmat A, Masudulla K, Farid O, Mahboob A. 2023. Exploring

the nano-fungicidal efficacy of green synthesized magnesium oxide nanoparticles (MgO NPs) on the development, physiology, and infection of carrot (*Daucus carota* L.) with *Alternaria* leaf blight (ALB): Molecular docking. *Journal of Integrative Agriculture*, **22**, 3069–3080.

Ajmal M, Hussain A, Ali A, Chen H, Lin H. 2022. Strategies for controlling the sporulation in *Fusarium* spp. *Journal of Fungi*, **9**, 10.

Akram W, Anjum T, Ahmad A. 2014. Basal susceptibility of tomato varieties against different isolates of *Fusarium oxysporum* f. sp. *lycopersici*. *International Journal of Agriculture and Biology*, **16**, 171–176.

Alexandru M, Lipșa F D, Florea A M, Ulea E. 2020. Analysis of mycotoxins from cereals and cereal products at Iasi county. *Agronomy Series of Scientific Research/Lucrri Tiinifice Seria Agronomie*, **63**, 209.

Ambreen M, Khan A, Raza A, Hussain T, Ali H. 2023. Unleashing the potential of carbon nanotubes for production of medicinal metabolites in *Nigella sativa* adventitious roots. *Plant Cell, Tissue and Organ Culture* (PCTOC), **155**, 581–601.

Ashraf H, Anjum T, Riaz S, Ahmad I S, Irudayaraj J, Javed S, Qaiser U, Naseem S. 2021. Inhibition mechanism of green-synthesized copper oxide nanoparticles from *Cassia fistula* towards *Fusarium oxysporum* by boosting growth and defense response in tomatoes. *Environmental Science* (Nano), **8**, 1729–1748.

Azizi-Lalabadi M, Hashemi H, Feng J, Jafari S M. 2020. Carbon nanomaterials against pathogens; the antimicrobial activity of carbon nanotubes, graphene/graphene oxide, fullerenes, and their nanocomposites. *Advances in Colloid and Interface Science*, **284**, 102250.

Bienert G P, Møller A L, Kristiansen K A, Schulz A, Møller I M, Schjoerring J K, Jahn T P. 2007. Specific aquaporins facilitate the diffusion of hydrogen peroxide across membranes. *Journal of Biological Chemistry*, **282**, 1183–1192.

Chen J N, Wu L T, Kun S, Zhu Y S, Ding W. 2022. Nonphytotoxic copper oxide nanoparticles are powerful “nanoweapons” that trigger resistance in tobacco against the soil-borne fungal pathogen *Phytophthora nicotianae*. *Journal of Integrative Agriculture*, **21**, 3245–3262.

Ding L, Wang H, Liu D, Zeng X A, Mao Y. 2020. Bacteria capture and inactivation with functionalized multi-walled carbon nanotubes (MWCNTs). *Journal of Nanoscience and Nanotechnology*, **20**, 2055–2062.

Dubey R, Dutta D, Sarkar A, Chattopadhyay P. 2021. Functionalized carbon nanotubes: Synthesis, properties and applications in water purification, drug delivery, and material and biomedical sciences. *Nanoscale Advances*, **3**, 5722–5744.

Ekwomadu T I, Mwanza M. 2023. Fusarium fungi pathogens, identification, adverse effects, disease management, and global food security: A review of the latest research. *Agriculture*, **13**, 1810.

Farhana A, Jenifer Selvarani A, Samrot A V, Alsrhani A, Raji P, Sahithya C S, Jane Cypriyana P, Senthilkumar P, Ling M P, Yishak S. 2022. Utilization of superparamagnetic iron oxide nanoparticles (SPIONs) impregnated activated carbon for removal of hexavalent chromium. *Journal of Nanomaterials*, **2022**, 1–13.

Galano A, Francisco-Márquez M, Alvarez-Idaboy J R. 2011. Canolol: A promising chemical agent against oxidative stress. *The Journal of Physical Chemistry B*, **115**, 8590–8596.

Mc Gee D, Archer L, Smyth T J, Fleming G T A, Touzet N. 2020. Bioprospecting and LED-based spectral enhancement of antimicrobial activity of microalgae isolated from the west of Ireland. *Algal Research*, **45**, 101704.

González-García Y, Cadenas-Pliego G, Alpuche-Solís Á G, Cabrera R I, Juárez-Maldonado A. 2021. Carbon nanotubes decrease the negative impact of *Alternaria solani* in tomato crop. *Nanomaterials*, **11**, 1080.

González-García Y, Cadenas-Pliego G, Alpuche-Solís Á G, Cabrera R I, Juárez-Maldonado A. 2022. Effect of carbon-based nanomaterials on Fusarium wilt in tomato. *Scientia Horticulturae*, **291**, 110586.

Gurunathan S, Lee A R, Kim J H. 2022. Antifungal effect of nanoparticles against COVID-19 linked black fungus: A perspective on biomedical applications. *International Journal of Molecular Sciences*, **23**, 12526.

Hafiz A H, Jun Z, Yu-shuang G, Mei-xu G, Wei G. 2022. Proteomic analysis of pathogen-responsive proteins from maize stem apoplast triggered by *Fusarium verticillioides*. *Journal of Integrative Agriculture*, **21**, 446–459.

Helal S H, Abdel-Aziz H M, El-Zayat M M, Hasaneen M N. 2022. Preparation, characterization and properties of three different nanomaterials either alone or loaded with nystatin or fluconazole antifungals. *Scientific Reports*, **12**, 22110.

Ibrahim M I, Alamry K A, Hussein M A, Alsafadi D, Rafatullah M. 2023. An efficient antimicrobial performance of hybrid functionalized MWCNTs/GNPts bionanocomposites based on poly (3-hydroxybutyrate-co-3-hydroxyvalerate). *Chemistry Select*, **8**, e202205011.

Ibrahim S R M, Sirwi A, Eid B G, Mohamed S G A, Mohamed G A. 2021. Bright side of *Fusarium oxysporum*: Secondary metabolites bioactivities and industrial relevance in biotechnology and nanotechnology. *Journal of Fungi* (Basel), **7**, 943.

Isgoren M, Gengec E, Veli S, Hassandoost R, Khataee A. 2023. The used automobile catalytic converter as an efficient catalyst for removal of malathion through wet air oxidation process. *International Journal of Hydrogen Energy*, **48**, 6499–6509.

Jun L Y, Mubarak N, Yon L S, Bing C H, Khalid M, Abdullah E. 2018. Comparative study of acid functionalization of carbon nanotube *via* ultrasonic and reflux mechanism. *Journal of Environmental Chemical Engineering*, **6**, 5889–5896.

Kang J B, Zhang J, Liu Y K, Song J C, Ou J L, Xian T, Zhou M G, Duan Y B. 2023. Mitochondrial dynamics caused by QoIs and SDHIs fungicides depended on FgDnm1 in *Fusarium graminearum*. *Journal of Integrative Agriculture*, **22**, 481–494.

Khalid A, Madni A, Raza B, Islam M ul, Hassan A, Ahmad F, Ali H, Khan T, Wahid F. 2022. Multiwalled carbon nanotubes functionalized bacterial cellulose as an efficient healing material for diabetic wounds. *International Journal of Biological Macromolecules*, **203**, 256–267.

Kovač T, Borišev I, Kovač M, Lončarić A, Čačić Kenjerić F, Djordjevic A, Strelec I, Ezekiel C N, Sulyok M, Krska R. 2020a. Impact of fullerol C60 (OH) 24 nanoparticles on the production of emerging toxins by *Aspergillus flavus*. *Scientific Reports*, **10**, 725.

Kovač T, Šarkanj B, Borišev I, Djordjevic A, Jović D, Lončarić A, Babić J, Jozinović A, Krska T, Gangl J. 2020b. Fullerol c60 (oh) 24 nanoparticles affect secondary metabolite profile of important foodborne mycotoxigenic fungi *in vitro*. *Toxins*, **12**, 213.

Krithika T, Iswarya T, Sowndarya T. 2023. Introduction of nanohybrid materials. In: *Nanohybrid Materials for Treatment of Textiles Dyes*. Springer Nature, Singapor. pp. 1–17.

Li C H, Fan Z L, Huang X Y, Wang Q H, Jiang C, Xu J R, Jin Q J. 2022. Mutations in FgPrp6 suppressive to the Fgprp4 mutant in *Fusarium graminearum*. *Journal of Integrative Agriculture*, **21**, 1375–1388.

Liu L, Jin X, Lu X, Guo L, Lu P, Yu H, Lv B. 2023. Mechanisms of surfactin from *Bacillus subtilis* SF1 against *Fusarium foetens*: A novel pathogen inducing potato wilt. *Journal of Fungi*, **9**, 367.

Maksimova Y, Bykova Y, Maksimov A. 2022. Functionalization of multi-walled carbon nanotubes changes their antibiofilm and probiofilm effects on environmental bacteria. *Microorganisms*, **10**, 1627.

Malekinejad F, Fink-Gremmels J, Malekinejad H. 2023. Zearalenone and its metabolite exposure directs oestrogen metabolism towards potentially carcinogenic metabolites in human breast cancer MCF-7 cells. *Mycotoxin Research*, **39**, 45–56.

Matras E, Gorczyca A, Pociecha E, Przemieniecki S W, Oćwieja M. 2022. Phytotoxicity of silver nanoparticles with different surface properties on monocots and dicots model plants. *Journal of Soil Science and Plant Nutrition*, **22**, 1647–1664.

Nandhini R S, Nithya R N, Vidhya K. 2021. GC-MS analysis of Phytochemical compounds in different extracts of *Curculigo orchiodes*. *Research Journal of Pharmacy and Technology*, **14**, 4355–4360.

Nelsen M P, Gargas A. 2008. Phylogenetic distribution and evolution of secondary metabolites in the lichenized fungal genus *Lepraria* (Lecanorales: Stereocaulaceae). *Nova Hedwigia*, **86**, 115–132.

Ntemafack A, Ali S, Dzelamonyuy A, Manhas R S, Atsafack S S, Kuiate J R, Waffo A B, Chaubey A. 2023. Chemical profile, biological potential, bioprospection and biotechnological application of endophytes of Rumex: A systematic review. *Industrial Crops and Products*, **195**, 116474.

Pariona N, Mtz-Enriquez A I, Sánchez-Rangel D, Carrión G, Paraguay-Delgado F, Rosas-Saito G. 2019. Green-synthesized copper nanoparticles as a potential antifungal against plant pathogens. *RSC Advances*, **9**, 18835–18843.

Poleto L, da Rosa L O, Fontana R C, Rodrigues E, Poletto É, Baldo G, Paesi S, Sales-Campos C, Camassola M. 2021. Production of antimicrobial metabolites against pathogenic bacteria and yeasts by Fusarium oxysporum in submerged culture processes. *Bioprocess and Biosystems Engineering*, **44**, 1321–1332.

Rahman M A, Abul Barkat H, Harwansh R K, Deshmukh R. 2022. Carbon-based nanomaterials: Carbon nanotubes, graphene, and fullerenes for the control of burn infections and wound healing. *Current Pharmaceutical Biotechnology*, **23**, 1483–1496.

Ramadan S M, Haleem R A J. 2023. Identification and phylogeny analysis of two new fusarium species causing dry rot on potato tubers in iraq. *Journal of Duhok University*, **26**, 79–86.

Rees D O, Bushby N, Cox R J, Harding J R, Simpson T J, Willis C L. 2007. Synthesis of [1,2-13C2,15N]-l-Homoserine and its incorporation by the PKS-NRPS system of fusarium moniliforme into the mycotoxin fusarin C. *ChemBioChem*, **8**, 46–50.

Rosengaus R, Traniello J, Lefebvre M, Maxmen A. 2004. Fungistatic activity of the sternal gland secretion of the dampwood termite *Zootermopsis angusticollis*. *Insectes Sociaux*, **51**, 259–264.

Safdar M, Kim W, Park S, Gwon Y, Kim Y O, Kim J. 2022. Engineering plants with carbon nanotubes: A sustainable agriculture approach. *Journal of Nanobiotechnology*, **20**, 275.

Saleemi M A, Fouladi M H, Yong P V C, Wong E H. 2020. Elucidation of antimicrobial activity of non-covalently dispersed carbon nanotubes. *Materials*, **13**, 1676.

Saleemi M A, Kong Y L, Yong P V C, Wong E H. 2022. An overview of antimicrobial properties of carbon nanotubes-based nanocomposites. *Advanced Pharmaceutical Bulletin*, **12**, 449.

Saleemi M A, Lim V. 2022. Overview of antimicrobial polyurethane-based nanocomposite materials and associated signalling pathways. *European Polymer Journal*, **167**, 111087.

Salem S S, Hashem A H, Sallam A A M, Doghish A S, Al-Askar A A, Arishi A A. Shehabeldine A M. 2022. Synthesis of silver nanocomposite based on carboxymethyl cellulose: Antibacterial, antifungal and anticancer activities. *Polymers*, **14**, 3352.

Santos T R, Andrade M B, Silva M F, Bergamasco R, Hamoudi S. 2019. Development of α- and γ-Fe2O3 decorated graphene oxides for glyphosate removal from water. *Environmental Technology*, **40**, 1118–1137.

Sanukrishna S, Jose V M. 2022. Evaluation of thermal and rheological characteristics of CNT-PAG nanolubricant for the development of energy efficient refrigeration systems. *Materials Today* (Proceedings), **58**, 114–120.

Shams A H, Helaly A A, Algeblawi A M, Awad-Allah E F. 2023. Efficacy of seed-biopriming with trichoderma spp. and foliar spraying of ZnO-nanoparticles induce cherry tomato growth and resistance to fusarium wilt disease. *Plants*, **12**, 3117.

Shoukat R, Khan M I. 2022. Carbon nanotubes/nanofibers (CNTs/CNFs): A review on state of the art synthesis methods. *Microsystem Technologies*, **28**, 885–901.

Siddiqui Z A, Hashmi A, Khan M R, Parveen A. 2020. Management of bacteria *Pectobacterium carotovorum*, *Xanthomonas campestris* pv. *carotae*, and fungi *Rhizoctonia solani*, *Fusarium solani* and *Alternaria dauci* with silicon dioxide nanoparticles on carrot. *International Journal of Vegetable Science*, **26**, 547–557.

da Silva Santos A C, Diniz A G, Tiago P V, de Oliveira N T. 2020. Entomopathogenic Fusarium species: A review of their potential for the biological control of insects, implications and prospects. *Fungal Biology Reviews*, **34**, 41–57.

Soffian M S, Halim F Z A, Aziz F, Rahman M A, Amin M A M, Chee D N A. 2022. Carbon-based material derived from biomass waste for wastewater treatment. *Environmental Advances*, **9**, 100259.

Stegarescu A, Lung I, Ciorîță A, Kacso I, Opriș O, Soran M L, Soran A. 2022. The antibacterial properties of nanocomposites based on carbon nanotubes and metal oxides functionalized with azithromycin and ciprofloxacin. *Nanomaterials*, **12**, 4115.

Tardast Z, Iranbakhsh A, Ebadi M, Ardebili Z O. 2023. Carboxylic acid-functionalized multiwalled carbon nanotubes (COOH-MWCNTs) improved production of atropine in callus of Datura inoxia by influencing metabolism, gene regulation, and DNA cytosine methylation; an in vitro biological assessment. *Plant Physiology and Biochemistry*, **202**, 107975.

Tewari C, Tatrari G, Kumar S, Pathak M, Rawat K S, Kim Y N, Saha B, Jung Y C, Mukhopadhyay P, Sahoo N G. 2023. Can graphene-based composites and membranes solve current water purification challenges-a comprehensive review. *Desalination*, 116952.

Thamer F H, Thamer N. 2023. Gas chromatography–Mass spectrometry (GC-MS) profiling reveals newly described bioactive compounds in *Citrullus colocynthis* (L.) seeds oil extracts. *Heliyon*, **6**, 9.

Thirugnanasambandan T, Gopinath S C. 2023. Nanomaterials in food industry for the protection from mycotoxins: An update. *3 Biotech*, **13**, 64.

Wale S, Platt B, Cattlin N D. 2008. *Diseases*, *Pests and Disorders of Potatoes*: *A Colour Handbook*. Elsevier.

Wang X, Zhou Z, Chen F. 2017. Surface modification of carbon nanotubes with an enhanced antifungal activity for the control of plant fungal pathogen. *Materials*, **10**, 1375.

Yadav A, Yadav K, Abd-Elsalam K A. 2023. Exploring the potential of nanofertilizers for a sustainable agriculture. *Plant Nano Biology*, **5**, 100044.

Yassin M T, Mostafa A A F, Al-Askar A A, Alkhelaif A S. 2022. *In vitro* antimicrobial potency of Elettaria cardamomum ethanolic extract against multidrug resistant of food poisoning bacterial strains. *Journal of King Saud University-Science*, **34**, 102167.

Yu W Y, Mei L, Yan H J, Wang J J, Zhang S M, Lu G D, Wang Z H, Shim W B. 2022. The peroxisomal matrix shuttling receptor Pex5 plays a role in FB1 production and virulence in *Fusarium verticillioides*. *Journal of Integrative Agriculture*, **21**, 2957–2972.

Yu Z, Li Q, Wang J, Yu Y, Wang Y, Zhou Q, Li P. 2020. Reactive oxygen species-related nanoparticle toxicity in the biomedical field. *Nanoscale Research Letters*, **15**, 115.

Zhang X Z, Chen S, Abubakar Y S, Mao X Z, Miao P F, Wang Z H, Zhou J, Zheng H W. 2023. FgGyp8 as a putative FgRab1 GAP is required for growth and pathogenesis by regulating FgSnc1-mediated secretory vesicles fusion in *Fusarium graminearum*. *Journal of Integrative Agriculture*, **22**, 3444–3457.

Executive Editor-in-Chief Fanghao Wan
Managing Editor Juan Zhang